A simple stochastic model for the feedback circuit between p16INK4a and p53 mediated by 38MAPK: Implications for senescence and apoptosis

Journal:	*Molecular BioSystems*
Manuscript ID:	MB-ART-04-2015-000230.R2
Article Type:	Paper
Date Submitted by the Author:	29-Jul-2015
Complete List of Authors:	de Oliveira, Luciana; Universidade Federal de Santa Maria, Physics Mombach, Jose; Universidade Federal de Santa Maria, Physics Castellani, Gastone; University of Bologna, Physics dept

A simple stochastic model for the feedback circuit between p16INK4a and p53 mediated by p38MAPK: Implications for senescence and apoptosis†

L. R. de Oliveira,*[a] J. C. M. Mombach,[a] and G. Castellani [b]

Received Xth XXXXXXXXXX 20XX, Accepted Xth XXXXXXXXX 20XX
First published on the web Xth XXXXXXXXXX 200X
DOI: 10.1039/b000000x

The mechanisms leading to the cell fate decision between apoptosis or senescence upon DNA damage are still unclear and have stochastic features. Cellular oxidative stress can generate DNA damage and activate the important mitogen-activated protein kinase 14 (p38MAPK) that is involved in pathologies like Alzheimer's. Based on experimental evidences we propose a simple network that might operate at the core of the cell control machinery for the choice between apoptosis and senescence involving the cross talk between p38MAPK, the tumor suppressor protein p53 and the cyclin-dependent kinase inhibitor (p16INK4a). We have performed two types of analysis, deterministic and stochastic, exploring the system's parameter space, in the first, we calculated the fixed points of the deterministic model and, in the second, we numerically integrated the master equation for the stochastic version. The model shows a variety of behaviors dependent on the parameters including states of high expression levels of p53 or p16INK4a that can be associated to an apoptotic or senescent phenotype, respectively, in agreement with experimental data. In addition, we observe both, monostable and bistable behavior (where bistability is a phenomenon in which two stable steady states coexist for a fixed set of control parameter values) which here we suggest to be involved the cell fate decision problem.

1 Introduction

DNA damage activates cell cycle checkpoints to arrest growth and promote DNA repair or to induce senescence or cell death[1]. Apoptotic mechanisms are well established, however the mechanisms driving the decision between these different cell fates are still unclear (e.g.,[2,3]). In particular, there is a growing interest to understand the connection between cellular senescence[4] and apoptosis[5]. Recent discoveries have extended the role of senescence as an anti-cancer mechanism to its involvement in other important biological processes such as aging, development and tissue repair[5]. Senescence is also involved in other diseases, but whether its contribution is beneficial or detrimental is not yet determined[5]. So, the study of senescence is essential to understand cell fate decisions, development and aging diseases.

In general, the molecular pathways that trigger senescence are pathology dependent but can be grouped in two cases: DNA damage or developmental programs[5]. In case of DNA damage-induced senescence an important case is stress-induced senescence generated by reactive oxigen species (ROS) that are involved in sarcopenia and Alzheimer's disease related to p38 mitogen-activated protein kinase (p38MAPK) activation[3,5–9]. ROS causes cellular oxidative stress and DNA damage that activate the p38MAPK pathway involving the p38 family of proteins (p38α-δ) in which p38α (here referred simply as p38MAPK) has a major role[10]. p38MAPK is known to induce senescence in human and mouse fibroblasts[11–13] through upregulation of the cyclin-dependent kinase inhibitor 2A (p16INK4a) blocking proliferation irreversibly[3,14,15]. In human cells senescence requires activation of the p38MAPK-p16INK4a and/or p53-cyclin-dependent kinase inhibitor 1A (p21) pathways (see figure 1).

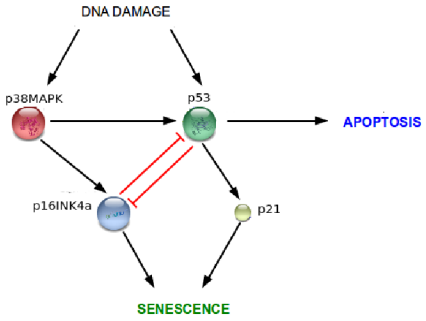

Fig. 1 DNA damage caused by ROS activates p38MAPK and p53 which can induce apoptosis or senescence (through p16INK4a and/or p21). Pointed and hammerheads arrows represent activatory and inhibitory interactions, respectively. The present model considers the p38MAPK-p16INK4a pathway to senescence.

p16INK4a is an important marker of senescent cells *in vivo* and *in vitro*[6,11,13,16,17] and p16INK4a gain of function experiments have shown that it causes senescent-like changes including increase of cell volume and expression of β-galactosidase[17]. The detailed molecular mechanisms of stress-induced senescence are not completely described but p38MAPK can derepress the CDKN2A gene locus that alternatively splices p16INK4a (and the alternate reading frame 14 or p14ARF)[18,19]. p38MAPK is also involved in apoptosis, its inhibition has pro-survival effects in cells treated with anticancer agents[20]. Recently, Kracikova et al.[21] showed that apoptosis is triggered when p53 accumulation reaches a threshold and since p38MAPK can activate p53[22–25], they both affect apoptosis regulation. In addition, p53 affects p16INK4a expression as shown in[26,27]. These facts suggest that these proteins are involved in the cell fate decision problem between apoptosis and senescence which seems to be stochastic, possibly bistable[28].

The traditional way to model this kind of biochemical network is through deterministic approaches: where the state of the system at any particular instant of time is regarded as a vector (or list) of amounts or concentrations and the changes are assumed to occur by a continuous process that is computed using the ordinary differential equations (ODE)[29–31]. However, this approach does not consider the effect of fluctuations, very large populations can be described by differential equations but as long as the system size is below $N = 10^3 \sim 10^4$ a more realistic mathematical framework is required. The natural framework is provided by Markov processes and the Master equation (ME) that describe the temporal evolution of the probability of each state specified by the number of units of each species. It is an equivalent form of the Chapman-Kolmogorov equation for Markov process, but it is easier to handle and more directly related to physical concepts[32,33]. Our interest here is to propose a simple stochastic model of cell fate decision involving the regulatory feedback circuit between p53 and p16INK4a regulated by p38MAPK that affects the decision between apoptosis or senescence. Experimental evidences show that senescence and apoptosis are interconnected, compensating each other.[5].

2 Cross-talk between p53 and p16INK4a regulated by p38MAPK

When we are dealing with the mathematical description of the cell cycle regulation even a minimal portion of a biochemical network is difficult to describe. Regarding the problem of cell fate decision upon DNA damage, there are many works dealing with cell survival and death, most of them consider the deterministic description, as in the works of Purvis[28], Wee[31], Ciliberto[34] or Batchelor[35] and others consider the stochastic description as in the work of Outtarra[36]. However, stochastic approaches using the ME are still scarce in the field. In this way, we address our problem in the qualitative network (derived from the more general network in figure 1) considering only the interactions between p53, p38MAPK and p16INK4a. In the network, shown in figure 2, "arrows" and "hammerheads" represent activatory and inhibitory interactions, respectively. The dashed line represents phosporylation mechanisms. In more detail, p38MAPK can phosphorylate p53[12,37] or (indirectly) induce p16INK4a[38]; p16INK4a can inhibit p53[39] inhibiting apoptosis; p53 can inhibit p16INK4a[38] inhibiting senescence. In what follows we describe the mathematical methods.

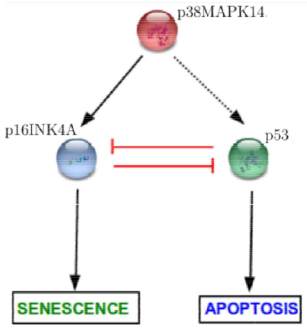

Fig. 2 Minimal model network for cell fate decision between apoptosis and senescence. In this qualitative network, "arrows" and "hammerheads" represent activatory and inhibitory interactions, respectively, and the dashed line represents phosporylation mechanisms.

2.1 Deterministic approach

Techniques to derivate the differential equations from the interactions between the components of biological networks are well established (for further information see, for example, references[30,31,40,41]). Here we investigate the dynamical properties of the simple model represented in figure 2. A further representation of the system may be done by the abstract kinetic model shown in figure 3, where p53, p53* and p16INK4a stand for the concentration of p53, phosphorylated p53 and p16INK4a, respectively. To take advantage of the quasi-stationary approximation[29,42], we will consider the total concentration of p53 is constant,

$$[p53_{tot}] = [p53] + [p53^*] \quad (1)$$

which is reasonable with the timescale typical of phosphorylation and dephosphorylation events on the order of seconds. The activation of p53* occurs much faster than the transcriptional, translational, and degradation processes involving p53

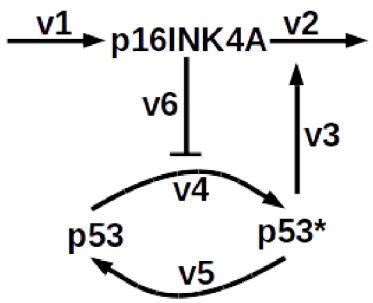

Fig. 3 Abstract kinetic model for the cross talk between p53 and p16INK4a. In figure, p53, p53* and p16INK4a stand for concentration of p53, phosphorylated p53 and p16INK4a, respectively.

on the time scale of hours[35,43,44]. In this way, we can describe the system as

$$\frac{d[p16INK4a]}{dt} = v_1 - v_2 - v_3$$

$$\frac{d[p53^*]}{dt} = v_4 - v_5 - v_6. \qquad (2)$$

The detailed description of the model can be found in Appendix A and it can be interpreted in the following way: p16INK4a is activated by p38MAPK with a rate v_1 and the degradation of p16INK4a is divided in two parts: v_2, the p53-independent degradation and v_3, the p53-dependent decay. p38MAPK also activates the phosphorylation of p53 with a rate v_4 and the amount of $p53^*$ can decrease in two ways: v_5 the p16INK4a-independent deactivation and v_6 the p16INK4a-dependent inhibition.

We choose to express the equations in terms of [p16INK4a] and [$p53^*$] and to have normalized mean field equations we write

$$\phi_x = [p16INK4a]/N_x \qquad (3)$$

and

$$\phi_y = [p53^*]/N_y \qquad (4)$$

where N_x is the total concentration of [p16INK4a] and N_y is [$p53_{tot}$], then the system is completely described by equations

$$\frac{d\phi_x}{dt} = \frac{k_0}{N_x} - k_d\phi_x - \frac{Nyk_2\phi_x\phi_y}{j_2 + N_x\phi_x}$$

and

$$\frac{d\phi_y}{dt} = \frac{k_1(1-\phi_y)}{j_1 + N_y(1-\phi_y)} - \frac{k_{m1}\phi_y}{j_{m1} + N_y\phi_y} - \frac{k_{m3}N_x\phi_x\phi_y}{j_{m3} + N_y\phi_y} \qquad (5)$$

Equations (5) determine the stable points of the deterministic version and also allow to write the ME for the stochastic description.

2.2 Stochastic approach

In general, the term 'master equation' is associated with a set of equations that describe the temporal evolution of the probability of a particular system. The system evolves and asymptotically reaches a stationary equilibrium after a specific relaxation time. The deterministic approach does not determine uniquely the ME since the nature of the noise needs to be specified[32]. In our case, the two-dimensional ME describes the problem as a function of the concentration of p16INK4a and p53:

$$\dot{p}(n_x,n_y,t) = (E_{n_x} - 1)r_{n_x}p(n_x,n_y) + (E_{n_x}^{-1} - 1)g_{n_x}p(n_x,n_y)$$
$$+(E_{n_y} - 1)r_{n_y}p(n_x,n_y) + (E_{n_y}^{-1} - 1)g_{n_y}p(n_x,n_y), \qquad (6)$$

where we are assuming the convention for the variables: ϕ_x, ϕ_y for the deterministic approach and n_x, n_y for the stochastic approach. The interpretation of the ME (6) is that the probability $p(n_x,n_y,t)$ to have n_x molecules of p16INK4a and n_y molecules of p53 at time t is written in terms of the gain due to the transitions from n_{i-1} to n_i denoted by g_{n_i}, and the loss due to the transitions from n_i to n_{i-1} denoted by r_{n_i}, with $i = x,y$. This ME is derived under the condition of a one-step Poisson process[32] and the terms E_{n_i} and $E_{n_i}^{-1}$ are the 'step operator' or 'van Kampen operator' and their effect on an arbitrary function $f(n_i)$ is

$$E_{n_i}f(n_i) = f(n_i+1) \quad \text{and} \quad E_{n_i}^{-1}f(n_i) = f(n_i-1). \qquad (7)$$

As shown in another work, the choice of the generation and recombination terms is arbitrary and different master equations can have the same mean field limit[45]. Considering the mean field equations (5), our choice for the terms associated with the n_x and n_y are:

$$g_{n_x} = \frac{k_0}{N_x} \qquad r_{n_x} = k_d n_x + \frac{Nyk_2 n_x n_y}{j_2 + N_x n_x} \qquad (8)$$

$$g_{n_y} = \frac{k_1(1-n_y)}{j_1 + N_y(1-n_y)} \qquad r_{n_y} = \frac{k_{m1}n_y}{j_{m1} + N_y n_y} + \frac{k_{m3}N_x n_x n_y}{j_{m3} + N_y n_y}.$$

We are interested in equilibrium properties that are obtained from the stationary distribution $p^s(n_x,n_y)$. The methods to derive the stationary distribution are dependent on the fulfillment of the detailed balance (DB) condition. If the DB condition holds, it is possible to find the stationary distribution by iterating the method used for the one-dimensional ME[32], whereas if the DB is broken we have to take into account the correction arising from the presence of a 'nonconservative' term[46]. In any case, if the DB does not holds, the stationary distribution can be found numerically by computing the kernel of the transition matrix or by integrating the system (8) for a sufficiently long time[32]. The validity of this definition relies on the structure of the ME that does not contain diagonal terms

(i.e. there are no terms with simultaneous variations of n_x and n_y). To verify if the DB condition holds, we use the 'commutator' $C(n_x,n_y)$[46],

$$C(n_x,n_y)=\frac{g^{(n_y)}_{n_x-1,n_y-1}\cdot g^{(n_x)}_{n_x-1,n_y}}{r^{(n_y)}_{n_x-1,n_y}\cdot r^{(n_x)}_{n_x,n_y}}-\frac{g^{(n_x)}_{n_x-1,n_y-1}\cdot g^{(n_y)}_{n_x,n_y-1}}{r^{(n_x)}_{n_x,n_y-1}\cdot r^{(n_y)}_{n_x,n_y}}. \quad (9)$$

if $C(n_x,n_y)=0$, it holds, whereas if $C(n_x,n_y)\neq 0$, it does not hold.

3 Results

Unlike equilibrium idealized models, biological systems work far from equilibrium, a cell, for example, is an open system that exchange molecules and energy with its environment, but in its homeostatic state all concentrations and fluctuations are stationary. Therefore, modeling the stationary state is very useful to describe biological systems and in this way we are proposing the analysis of the agreement between the deterministic and stochastic approaches at stationary state. With the simplified model that we have described in section 2 we expect to have both, monostable and bistable systems. Monostability is characterized by one stable point in the deterministic approach and one peak in the stochastic distribution, which means that there is just one possible fate for the system: apoptosis or senescence. On the other hand, bistability presents two stable points and one unstable point in the deterministic approach, and a bimodal distribution in the stochastic case, which means the possibility of having two states: one associated to apoptosis and other to senescence. We compare the deterministic and stochastic approaches through the calculation of the fixed points (5) and numerical integration of the master equation (8), respectively. In the deterministic approach we have considered the phase space of the system at $t=t^s$, where t^s is the time when the system reaches the stationary state.

At time t^s, the system does not change anymore and it can be characterized by the fixed points that are solutions of the system

$$\frac{d\phi_x}{dt}=0 \qquad \textit{and} \qquad \frac{d\phi_y}{dt}=0. \quad (10)$$

The fixed points are functions of ϕ_x and ϕ_y, therefore, we can use this information to construct the phase space and for sake of simplicity we will present just results related with variable ϕ_y and plot the function $\frac{d\phi_y}{dt}$. The variable ϕ_x is trivially derived from ϕ_y: at stationary state we can write

$$\phi_x^s=\frac{1}{2k_d}\left(k_0-j_2k_d-k_2\phi_y^s+\sqrt{4j_2k_0k_d+(k_0-j_2k_d-k_2\phi_y)^2}\right),$$

which let us see how the derivative behaves and also determines in a very simple way the sign of the function at fixed points.

For our system represented by the equations (8) the detailed balance condition is not valid for any set of parameters that we have considered, therefore we are integrating the master equation and recognize the stable stationary state ($p^s(n_x,n_y)$) as the the point when the distribution probability does not change anymore. An important result that we considered is the maximum value of the stationary distribution is equivalent to the value of the stable points in the deterministic system, which let us compare the two approaches. We have a complete description of the behavior of the system based on equations of each approach and a detailed description of each parameter can be found in the table 1 of appendix A. From them we know how terms are related with production (activation and phosphorylation) or destruction (decay and dephosphorilation) of the components of the system. The relationship between different parameters is not trivial, but in a general way we can predict their behavior. The results are divided in two parts: 1) validation of the model: comparison with experimental results to verify if the model is able reproduce the phenotypes reported in literature and 2) study of the influence of the parameters in the behavior of the model and possible predictions about cellular phenotype.

3.1 Validation of the model

p53 and p16INK4a have a central importance in our model because the experimental data shows that high levels of p53 drive cells into apoptosis[47–49], while high levels of p16INK4a drive cells into senescence[11,50]. Using this information we can simulate in the models the overexpression of these proteins and also change other parameters according to biological knowledge. In the equations we identify that the principal parameter related to senescence is k_0, the rate of activation of p16INK4a by p38MAPK, while for apoptosis are k_1 and j_1 that are the rates of phosphorylation of p53 by p38MAPK and the Michaelis constant of phosphorylation of p53 by p38MAPK, respectively. In case of senescence, k_0 is linearly related to p16INK4a, contrastingly k_1 is linearly related to the phosphorylation of p53, but it is inversely related to j_1. The list of parameters considered is shown in Table 2 of Appendix A.

Analyzing the solution of the deterministic system (5) and using the parameters of Case 1 of Table 2 we found only one stable fixed point, $\phi_x=29.9224, \phi_y=0.1002$. Figure 4 exhibits the corresponding phase space plotted in terms of concentration ϕ_y. This result implies that the system is in the senescent state by equations (3) and (4), as the concentration of ϕ_y is almost null and all other molecules are concentrated in ϕ_x. When we consider the stochastic distribution (figure 5) we

see a more detailed scenario, since the probability is concentrated around $n_{max} \simeq \{30,0\}$ which corresponds to senescence as it is related n_x.

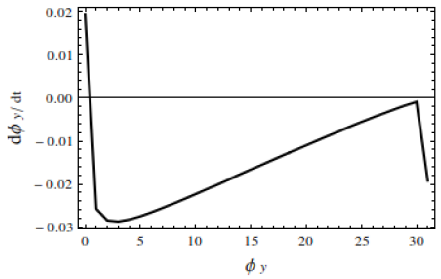

Fig. 4 Plot of the function $\frac{d\phi_y}{dt}(\phi_y)$ at $t = t^s$ with parameters values of Case 1 in Table 2 corresponding to senescence (overexpression of p16INK4a)[11,50] for deterministic approach. The fixed point is: $\phi_x = 29.9224, \phi_y = 0.1002$.

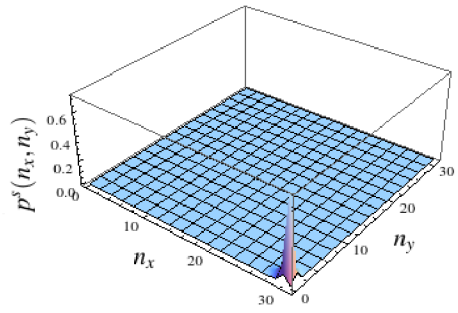

Fig. 5 Plot of the stationary distribution $p^s(n_x,n_y)$ with parameter values of Case 1 in Table 2 corresponding to senescence (overexpression of p16INK4a)[11,50] for stochastic approach. The initial condition used is $p(18,7,0) = 1$ for a system with dimensions $N_x = N_y = 31$.

The deterministic analysis of Case 2 in Table 2 yields again just one fixed stable point $\phi_x = 0.0007, \phi_y = 30.9502$ corresponding now to apoptosis. The concentration migrates from ϕ_x to ϕ_y (see figure 6). Similarly, the corresponding stationary distribution of the sthocastic model (figure 7) shows the probability concentration around the point $n_{max} \simeq \{0,30\}$ corresponding to apoptosis.

The results above tend to support the model and motivated us to explore different sets of parameters.

3.2 Model analysis

In the following we discuss the four cases listed in Table 3 of Appendix A for different sets of the parameters that yield interesting dynamic behavior, they were chosen in an arbitrary way.

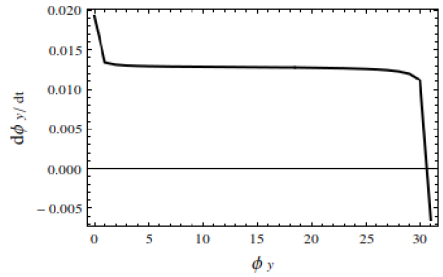

Fig. 6 Plot of the function $\frac{d\phi_y}{dt}(\phi_y)$ at $t = t^s$ with parameters values of Case 2 in Table 2 corresponding to apoptosis (overexpression of p53)[47–49] for deterministic approach. The fixed point is: $\phi_x = 0.0007, \phi_y = 30.9502$.

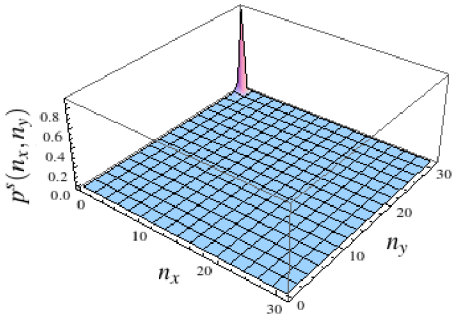

Fig. 7 Plot of the stationary distribution $p^s(n_x,n_y)$ with parameter values of Case 2 in Table 2 corresponding to apoptosis (overexpression of p53)[11,50] for stochastic approach. The initial condition used is $p(1,31,0) = 1$ for a system with dimensions $N_x = N_y = 31$.

Case 1: *Close agreement between deterministic and stochastic approaches.*

Mathematically the two approaches almost coincide: as shown in figure 8 the deterministic system shows just one stable fixed point at $\phi_x = 19.9798, \phi_y = 0.0262$ and the stationary distribution has just one peak with maximum at $n_{max} \simeq \{20,0\}$. Biologically this result can be interpreted as the only accessible state to the system is senescence, because the stable fixed point and the probability distribution have a significant concentration only for ϕ_x and n_x. This fact can be explained with the analysis of the parameters (for further details see Appendix A), in this case the production rate of $p16INK4a$ controlled by parameter k_0 is 10^2 times greater than the parameter related with the degradation of $p16INK4a$ controlled by k_d.

Case 2: *bistable behavior.*

In this case both approaches present favorable conditions for bistability, with apoptotic and senescent states accessible to the system. Mathematically, the deterministic approach shows three fixed points: two stable at $\phi_x = 0.1578, \phi_y = 30.9991$ and $\phi_x = 16.4121, \phi_y = 0.2954$ and one unstable at

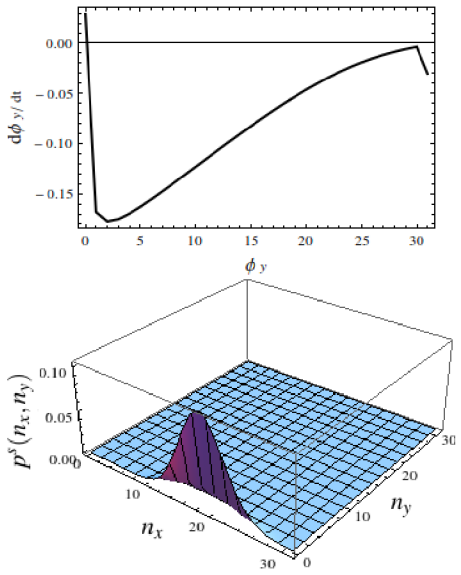

Fig. 8 Agreement between the deterministic and stochastic approaches for Case 1 in Table 3 of Appendix A. Top: Plot of the function $\frac{d\phi_y}{dt}(\phi_y)$ at $t = t^s$, showing that deterministic system has a single fixed point at $\phi_x = 19.9798, \phi_y = 0.0262$. Bottom: Plot of the stationary distribution of stochastic system shows a single peak. For the numerical simulation the initial condition used is $p(18,7,0) = 1$ and we have considered a system with dimension $N_x = N_y = 31$.

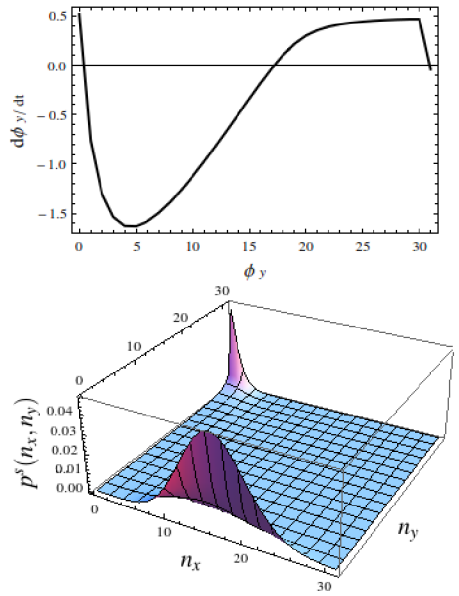

Fig. 9 Bistability in both deterministic and stochastic approaches for Case 2 in Table 3 of Appendix A. Top: Plot of the function $\frac{d\phi_y}{dt}(\phi_y)$ at $t = t^s$, in this case the deterministic system shows three fixed points: two stable points at $\phi_x = 0.1578, \phi_y = 30.9991$ and $\phi_x = 16.4121, \phi_y = 0.2954$ and one unstable point at $\phi_x = 2.3498, \phi_y = 17.2154$. Bottom: Plot of the stationary distribution of the stochastic system shows two peaks. For the numerical simulation the initial condition used is $p(18,7,0) = 1$ and we have considered a system with dimension $N_x = N_y = 31$.

$\phi_x = 2.3498, \phi_y = 17.2154$. While the stationary probability distribution shows a clear separation between senescent and apoptotic states (see figure 9), however the senescent state is more probable then the apoptotic. The analysis of the parameters suggests that higher production of p16INK4a (k_0) and higher phosphorylation of p53 (k_1) enable the system to a bistable behavior, but the low value of p16INK4a dependent degradation (k_2) can increase the probability of senescent states.

Case 3: *ghost effect.*

The deterministic system presents only one stable point at $\phi_x = 0.1092, \phi_y = 30.9977$, but we can clearly see a second peak in the stationary distribution in figure 10, where only the highest peak comes from a deterministic stable point. This kind of behavior was already observed also in other works [29,51] and the qualitative explanation is that the deterministic system is monostable but very close to the transition point in which the system becomes bistable. It is known that in these situations a ghost remains in the region where the stable point has disappeared. This behavior results in the presence of a peak in the stationary distribution of the corresponding stochastic systems, that remains bistable also when the deterministic system is not anymore. With the analysis of parameters we can see that the high value of k_d and low value of j_1 present in the production equation of p53* explain why the system exhibits only apoptotic states.

Case 4: *peak masking effect.*

In this case the two approaches do not agree: the deterministic approach shows three fixed points, two stable at $\phi_x = 0.1464, \phi_y = 30.9767$ and $\phi_x = 3.2310, \phi_y = 2.7426$ and one unstable at $\phi_x = 2.3638, \phi_y = 7.4063$, but the stationary distribution has only one peak (see figure 11). The stochastic distribution shows only the first stable point which has the largest basin of attraction, and the lower peak is masked. In simple terms, the lower state behaves like a sort of metastable state, as the states of the system with high protein level are visited only occasionally [29]. From the analysis of parameters we can see that a high value of k_1 and a small value of j_1 related to the production of p53* lead the system to an apoptotic state.

4 Conclusions

Senescence and apoptosis are functionally connected, however the mechanisms are yet unclear. Here we proposed a

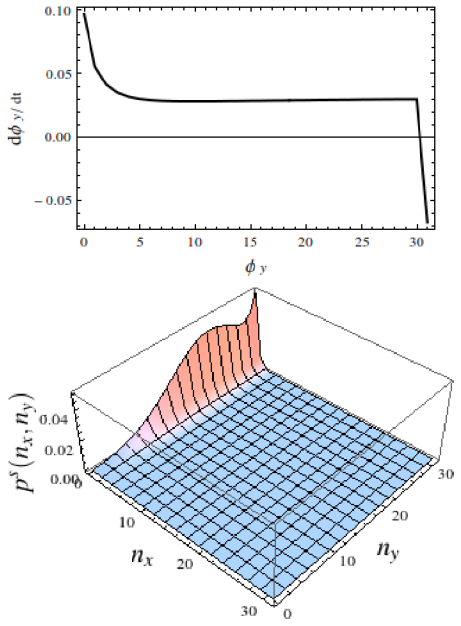

Fig. 10 'ghost effect' for Case 3 in Table 3 of Appendix A. Top: Plot of the function $\frac{d\phi_y}{dt}(\phi_y)$ at $t = t^s$, for the deterministic system showing a single stable point at $\phi_x = 0.1092, \phi_y = 30.9977$. Bottom: The stationary distribution of the stochastic system has two peaks. For the numerical simulation the initial condition used is $p(15,15,0) = 1$ and we have considered a system with dimension $N_x = N_y = 31$.

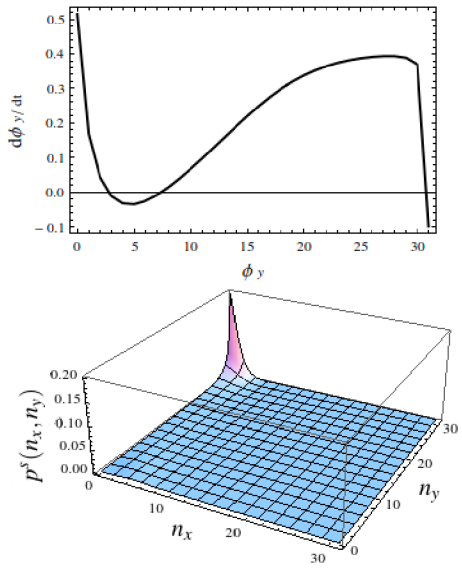

Fig. 11 Peak masking effect for Case 4 in Table 3 of Appendix A. Top: Plot of the function $\frac{d\phi_y}{dt}(\phi_y)$ at $t = t^s$ for deterministic system shows three fixed points: two stable at $\phi_x = 0.1464, \phi_y = 30.9767$ and $\phi_x = 3.2310, \phi_y = 2.7426$ and one unstable at $\phi_x = 2.3638, \phi_y = 7.4063$. Bottom: The stationary distribution of stochastic system has a single peak. For the numerical simulation the initial condition used is $p(1,15,0) = 1$ and we have considered a system with dimension $N_x = N_y = 31$.

negative feedback biochemical circuit between p16INK4a-p53 activated by p38MAPK that is able to describe the cell fate decisions between apoptosis and senescence that presents bistable behavior.

We used deterministic and stochastic approaches to model the circuit through determination of the fixed points in the deterministic case and numerical integration of the master equation in the stochastic case. In general, the stochastic method has advantages in relation to the deterministic one for allowing the calculation of state probabilities. The model matches experimental results related to the overexpression of p53 and p16INK4a associated with apoptotic and senescent states, respectively. When we analyze other parameter combinations we find monostable and bistable behavior in both approaches and they agree in cases 1 and 2 in section 3.2 above, where we found that senescent states are more probable than apoptotic ones. On the other hand, substantial differences between the two approaches were observed in cases 3 and 4: (*i*) in case 3 the bistability found in the stochastic approach corresponds to a monostable state in the deterministic case and it can be explained by the presence of a ghost state in the deterministic system that generates a secondary peak in the stationary distribution; (*ii*) in case 4 the stochastic distribution has a single peak and the deterministic two stable fixed points. In both cases the only accessible state is apoptosis, which we interpret as a sort of anti-tumor mechanism since the system is near the transition from monostable to a bistable state leading to the appearance of metastable apoptotic states.

In summary, we argue that the presence of bistability in this type of circuits can explain the compensation between apoptosis and senescence[5] and the indeterminism in cell fate decisions.

Acknowledgments

We acknowledge financial support from the Brazilian agency CNPq (grants 402547/2012-8, 304805/2012-2) and G. Castellani acknowledges support from EU projects FibeBiotics (289517), Mission-T2D (600803) and Methods for Integrated analysis of multiple Omics datasets (MIMOmics) (305280).

References

1 A. Sancar, L. A. Lindsey-Boltz, K. Ünsal-Kaçmaz and S. Linn, *Annual review of biochemistry*, 2004, **73**, 39–85.

2 T. Kuilman, C. Michaloglou, W. J. Mooi and D. S. Peeper, *Genes & development*, 2010, **24**, 2463–2479.
3 J. C. Mombach, C. A. Bugs and C. Chaouiya, *BMC Genomics*, 2014, **15(Suppl 7)**, S7.
4 J. M. van Deursen, *Nature*, 2014, **509**, 439–446.
5 D. Muñoz-Espín and M. Serrano, *Nature reviews Molecular cell biology*, 2014, **15**, 482–496.
6 R. Bhat, E. P. Crowe, A. Bitto, M. Moh, C. D. Katsetos, F. U. Garcia, F. B. Johnson, J. Q. Trojanowski, C. Sell and C. Torres, *PLoS One*, 2012, **7**, e45069.
7 J. C. Mombach, B. Vendrusculo and C. A. Bugs, *Science*, 2015.
8 E. Edström, M. Altun, E. Bergman, H. Johnson, S. Kullberg, V. Ramírez-León and B. Ulfhake, *Physiology & Behavior*, 2007, **92**, 129–135.
9 D. J. Baker, T. Wijshake, T. Tchkonia, N. K. LeBrasseur, B. G. Childs, B. van de Sluis, J. L. Kirkland and J. M. van Deursen, *Nature*, 2011, **479**, 232–236.
10 T. M. Thornton and M. Rincon, *International journal of biological sciences*, 2009, **5**, 44.
11 J. Campisi, *Annual review of physiology*, 2013, **75**, 685–705.
12 J. Kwong, M. Chen, D. Lv, N. Luo, W. Su, R. Xiang and P. Sun, *Molecular and cellular biology*, 2013, **33**, 3780–3794.
13 J. Zhu, D. Woods, M. McMahon and J. M. Bishop, *Genes & development*, 1998, **12**, 2997–3007.
14 S. W. Lowe, H. E. Ruley, T. Jacks and D. E. Housman, *Cell*, 1993, **74**, 957–967.
15 M. Hollstein, D. Sidransky, B. Vogelstein and C. C. Harris, *Science*, 1991, **253**, 49–53.
16 F. Zindy, D. E. Quelle, M. F. Roussel and C. J. Sherr, *Oncogene*, 1997, **15**, 203–211.
17 W. Wang, J. Wu, Z. Zhang and T. Tong, *Journal of Biological Chemistry*, 2001, **276**, 48655–48661.
18 M. Toshiyuki and J. C. Reed, *Cell*, 1995, **80**, 293–299.
19 K. Polyak, Y. Xia, J. L. Zweier, K. W. Kinzler and B. Vogelstein, *Nature*, 1997, **389**, 300–305.
20 R. Sanchez-Prieto, J. M. Rojas, Y. Taya and J. S. Gutkind, *Cancer research*, 2000, **60**, 2464–2472.
21 M. Kracikova, G. Akiri, A. George, R. Sachidanandam and S. Aaronson, *Cell Death & Differentiation*, 2013, **20**, 576–588.
22 V. Adler, M. R. Pincus, T. Minamoto, S. Y. Fuchs, M. J. Bluth, P. W. Brandt-Rauf, F. K. Friedman, R. C. Robinson, J. M. Chen, X. W. Wang *et al.*, *Proceedings of the National Academy of Sciences*, 1997, **94**, 1686–1691.
23 S. Y. Fuchs, V. Adler, T. Buschmann, Z. Yin, X. Wu, S. N. Jones and Z. Ronai, *Genes & development*, 1998, **12**, 2658–2663.
24 D. V. Bulavin, S. Saito, M. C. Hollander, K. Sakaguchi, C. W. Anderson, E. Appella and A. J. Fornace Jr, *The EMBO journal*, 1999, **18**, 6845–6854.
25 E. F. Wagner and Á. R. Nebreda, *Nature Reviews Cancer*, 2009, **9**, 537–549.
26 K. Yamakoshi, A. Takahashi, F. Hirota, R. Nakayama, N. Ishimaru, Y. Kubo, D. J. Mann, M. Ohmura, A. Hirao, H. Saya *et al.*, *The Journal of cell biology*, 2009, **186**, 393–407.
27 C. A. Schmitt, J. S. Fridman, M. Yang, S. Lee, E. Baranov, R. M. Hoffman and S. W. Lowe, *Cell*, 2002, **109**, 335–346.
28 J. E. Purvis, K. W. Karhohs, C. Mock, E. Batchelor, A. Loewer and G. Lahav, *Science*, 2012, **336**, 1440–1444.
29 E. Giampieri, D. Remondini, L. de Oliveira, G. Castellani and P. Lió, *Molecular BioSystems*, 2011, **7**, 2796–2803.
30 B. D. Aguda, Y. Kim, M. G. Piper-Hunter, A. Friedman and C. B. Marsh, *Proceedings of the National Academy of Sciences*, 2008, **105**, 19678–19683.
31 K. B. Wee and B. D. Aguda, *Biophysical journal*, 2006, **91**, 857–865.
32 N. G. Van Kampen, *Stochastic processes in physics and chemistry*, Elsevier, North Holland, 1992, vol. 1.
33 L. R. de Oliveira, G. Castellani and G. Turchetti, *Master equation: Biological Applications and Thermodynamic Descripition.*, Scholars Press, Germany, 2014, vol. 1.
34 A. Ciliberto, B. Novák and J. J. Tyson, *Cell cycle*, 2005, **4**, 488–493.
35 E. Batchelor, C. S. Mock, I. Bhan, A. Loewer and G. Lahav, *Molecular cell*, 2008, **30**, 277–289.
36 D. A. Ouattara, W. Abou-Jaoud and M. Kaufman, *Journal of Theoretical Biology*, 2010, **264**, 1177 – 1189.
37 M. Sayed, S. O. Kim, B. S. Salh, O.-G. Issinger and S. L. Pelech, *Journal of Biological Chemistry*, 2000, **275**, 16569–16573.
38 J. Kwong, L. Hong, R. Liao, Q. Deng, J. Han and P. Sun, *Journal of Biological Chemistry*, 2009, **284**, 11237–11246.
39 F. J. Stott, S. Bates, M. C. James, B. B. McConnell, M. Starborg, S. Brookes, I. Palmero, K. Ryan, E. Hara, K. H. Vousden *et al.*, *The EMBO journal*, 1998, **17**, 5001–5014.
40 T. S. Gardner, C. R. Cantor and J. J. Collins, *Nature*, 2000, **403**, 339–342.
41 B. B. Aldridge, J. M. Burke, D. A. Lauffenburger and P. K. Sorger, *Nature cell biology*, 2006, **8**, 1195–1203.
42 H. Qian and L. M. Bishop, *International journal of molecular sciences*, 2010, **11**, 3472–3500.
43 N. Geva-Zatorsky, N. Rosenfeld, S. Itzkovitz, R. Milo, A. Sigal, E. Dekel, T. Yarnitzky, Y. Liron, P. Polak, G. Lahav *et al.*, *Molecular systems biology*, 2006, **2**, year.
44 A. Loewer, E. Batchelor, G. Gaglia and G. Lahav, *Cell*, 2010, **142**, 89–100.
45 L. De Oliveira, C. Castellani and G. Turchetti, *Communications in Nonlinear Science and Numerical Simulation*, 2015, **20**, 461–468.
46 A. Bazzani, D. Remondini, N. Intrator and G. C. Castellani, *Neural Computation*, 2003, **15(7)**, 1621.
47 T. F. Burns, E. J. Bernhard and W. S. El-Deiry, *Oncogene*, 2001, **20**, 4601–4612.
48 P. Taneja, S. Zhu, D. Maglic, E. A. Fry, R. D. Kendig and K. Inoue, *Clinical Medicine Insights. Oncology*, 2011, **5**, 235.
49 K. Polyak, T. Waldman, T.-C. He, K. W. Kinzler and B. Vogelstein, *Genes & development*, 1996, **10**, 1945–1952.
50 W. Wang, J. X. Chen, R. Liao, Q. Deng, J. J. Zhou, S. Huang and P. Sun, *Molecular and cellular biology*, 2002, **22**, 3389–3403.
51 M. B. Elowitz, A. J. Levine, E. D. Siggia and P. S. Swain, *Science*, 2002, **297**, 1183–1186.

A Appendix

Here we present the detailed mathematical derivation of the deterministic model introduced in section 2.1 and the parameters values used in our study.

A.1 Mathematical derivation of the deterministic model and description of parameters

Considering the abstract model in figure 3 we can derive the following dynamical equations

$$\begin{aligned} \frac{d[p16INK4a]}{dt} &= v_1 - v_2 - v_3 \\ \frac{d[p53^*]}{dt} &= v_4 - v_5 - v_6 \end{aligned} \tag{11}$$

where each component represented in the following way:

$$v_1 = k_0$$

is the activation rate of p16INK4a by p38MAPK and it is assumed to have a constant value k_0.

$$v_2 = k_d \cdot [p16INK4a]$$

is the p53-independent degradation of p16INK4a.

$$v_3 = \frac{k_2 \cdot [p53^*] \cdot [p16INK4a]}{j_2 + [p16INK4a]}$$

is the p53-dependent decay rate of p16INK4a.

$$v_4 = \frac{k_1 \cdot [N_y - p53^*]}{j_1 + [N_y - p53^*]}$$

is the phosphorylation rate of p53 by p38MAPK assumed to have a Michaelis-Menten type expression.

$$v_5 = \frac{k_{m1} \cdot [p53^*]}{j_{m1} + [p53^*]}$$

is the deactivation rate of $p53^*$ assumed to have a Michaelis-Menten type expression.

$$v_6 = \frac{k_{m3} \cdot [p16INK4a] \cdot [p53^*]}{j_{m3} + [p53^*]}$$

is the inhibition rate of $p53^*$ induced by p16INK4a assumed to have a Michaelis-Menten type expression.

Then we have

$$\begin{aligned} \frac{d[p16INK4a]}{dt} &= k_0 - k_d \cdot [p16INK4a] - \frac{k_2 \cdot [p53^*] \cdot [p16INK4a]}{(j_2 + [p16INK4a])} \\ \frac{d[p53^*]}{dt} &= \frac{k_1 \cdot [N_y - p53^*]}{j_1 + [N_y - p53^*]} - \frac{k_{m1} \cdot [p53^*]}{j_{m1} + [p53^*]} - \frac{k_{m3} \cdot [p16INK4a] \cdot [p53^*]}{j_{m3} + [p53^*]}. \end{aligned} \quad (12)$$

Taking $\phi_x = [p16INK4a]/N_x$ and $\phi_y = [p53^*]/N_y$ where N_x is the total concentration of [p16INK4a] and N_y is $[p53_{tot}]$ then the mean field equations are

$$\frac{d\phi_x}{dt} = \frac{k_0}{N_x} - k_d \phi_x - \frac{Nyk_2 \phi_x \phi_y}{j_2 + N_x \phi_x}$$

and

$$\frac{d\phi_y}{dt} = \frac{k_1(1-\phi_y)}{j_1 + N_y(1-\phi_y)} - \frac{k_{m1}\phi_y}{j_{m1} + N_y\phi_y} - \frac{k_{m3}N_x\phi_x\phi_y}{j_{m3} + N_y\phi_y}. \quad (13)$$

That is the system we have considered in our study. In Table 1 we present a detailed description of the parameters.

Table 1 Model parameters.

Description	Parameter
p16INK4a activation by p38MAPK	$k_0\ (\mu M/min)$
Degradation of p16INK4a	$k_d\ (min^{-1})$
Phosphorylation of p53 by p38MAPK	$k_1\ (\mu M/min)$
Michaelis constant of p53 phosphorylation by p38MAPK	$j_1\ (\mu M)$
Dephosphorilation of p53*	$km_1\ (\mu M/min)$
p16INK4a dependent degradation of p53*	$k_2\ (min^-1)$
Michaelis constant of p16 degradation by p53*	$j_2\ (\mu M)$
Michaelis constant of p53* dephosphorilation	$jm_1\ (\mu M)$
Dephosphorilation of p53* by p16INK4a	$km3\ (\mu M/min)$
Michaelis constant of p53* dephosphorilation by p16INK4a	$jm3\ (\mu M)$

A.2 Set of parameters used in the study

Table 2 Parameters used in section 3.1.

Parameters	Case 1: Senescence	Case 2: apoptosis
$k_0\ (\mu M/min)$	1.5	0.1
$k_d\ (min^{-1})$	0.05	5
$k_1\ (\mu M/min)$	0.6	0.6
$j_1\ (\mu M)$	0.01	0.1
$km_1\ (\mu M/min)$	0.2	0.2
$k_2\ (min^-1)$	0.04	0.4
$j_2\ (\mu M)$	1	0.1
$jm_1\ (\mu M)$	0.1	0.1
$km3\ (\mu M/min)$	0.05	0.05
$jm3\ (\mu M)$	0.2	2

Table 3 Parameters used in section 3.2.

Parameters	Case 1	Case 2	Case 3	Case 4
$k_0\ (\mu M/min)$	1	15	7	15
$k_d\ (min^{-1})$	0.05	0.9	5	4
$k_1\ (\mu M/min)$	0.9	16	3	16
$j_1\ (\mu M)$	0.01	0.01	0.001	0.01
$km_1\ (\mu M/min)$	0.2	0.2	2	2
$k_2\ (min^-1)$	0.04	0.78	4	0.78
$j_2\ (\mu M)$	0.76	0.99	1.99	0.099
$jm_1\ (\mu M)$	0.1	0.1	1	0.1
$km3\ (\mu M/min)$	0.37	7.5	1.5	7.5
$jm3\ (\mu M)$	0.2	2	5	2